Bandgap Saturation in Room Temperature Synthesized Cobalt Doped ZnS Nanoparticles

Sujan Kumar Das[1], Shahnaj Parvin[1], Ummay Honey[1], Md. Sohel Rana[1], Nasrin Jewena[2], Jahirul Islam Khandaker[1] and Farid Ahmed[1]

1. Department of Physics, Jahangirnagar University, Savar, Dhaka-1342, Bangladesh

2. Department of Chemistry, Jahangirnagar University, Savar, Dhaka-1342, Bangladesh

Abstract: In this study, cobalt doped ZnS nanoparticles (NPs) have been synthesized by simple chemical precipitation method with six different weight percentages (0.0, 0.1, 0.3, 0.5, 0.7 and 1.0%) of cobalt content at room temperature (30 °C). X-ray diffraction (XRD) patterns of the samples revealed the formation of cubic structure and calculated particle size were found to be nano-sized. Optical band gap values have been obtained from UV-Vis absorption spectra. It has also been found that energy band gap (E_g) increases with the increase in molar concentration of reactant solution and the variation of bandgap was between 5.30-6.01 eV with cobalt doping.

Key words: ZnS, nanoparticles, cobalt doped, bandgap, precipitation method.

1. Introduction

Semiconducting nanoparticles such as metal sulfide and metal oxides are well recognized for their use in the optoelectronic field [1], solar cells, light-emitting diodes, sensors [2], etc. This kind of nanomaterials exhibits unusual physical and chemical properties in contrast with their bulk components, such as size-dependent modification of the bandgap energy. Doping impurities into nanoparticles is an effective approach for tuning their electronic, magnetic, constitutional, and optical properties for different desired applications [3]. In specific, when doped with magnetic ions (e.g. Mn^{2+}), these materials can develop unique magnetic and magnetooptical properties and provide unique opportunities for the advance field of spintronics [4].

ZnS is a large bandgap semiconductor material ($E_g \approx 3.68$ eV) which is commercially used in optoelectronics and likewise in thin film-based devices such as solar cells, ETM and HTM layers, and lasers [5]. Novel luminescence characteristics such as—durable and visible light emissions with distinctive colors were examined from doped ZnS nanoparticles at room temperature [6, 7]. Transition metal ion-doped semiconductor nanocrystals are acknowledged to show a nanosecond decay process, strong quantum efficiency, surface enhancement effect in clusters, and alteration of optical properties, all of which are greatly dependent on processing methods [8]. Transitional elements ions (e.g. Mn^{2+}, Ni^{2+}, and Cu^{2+} [9]) and rare-earth ions (e.g. Eu^{2+}) have been covered into ZnS nanostructures by thermal evaporation, sol-gel processing, Co-precipitation, microemulsion, etc. There are many papers on the photoluminescence properties of II-VI semiconductor nanoparticles doped with rare-earth ions [10]. There is limited work on photoluminescence studies of semiconductor nanoparticles co-stimulated with rare earth and transition metal ions [11]. This work purposes to synthesize pure ZnS and Co-doped ZnS nanoparticles and investigate their structural and optical properties. The effect of varying the concentration of cobalt chloride in ZnS nanoparticles

---

on the variety of bandgap and photovoltaic properties is also carefully explored to expand the usage of such type of doped material to optoelectronic devices especially solar cells.

Various studies implemented that the optoelectronic properties of ZnS nanoparticles shifted from its standard [12]. For instance, review of the optical properties of Eu-doped ZnS nanoparticles demonstrated that inter ionic transition occurs in the phase of Eu^{2+} [13]. Another report observed an orange emission in the Mn-doped ZnS nanoparticles [14]. Studies of Cu-doped ZnS nanoparticles [15] showed various luminescence peaks. So still there are some complications with doping with ZnS.

To reduce this kind of problem Co is adopted as the doping material in this report. It has been observed the doping of Co, generating influence on the energy level of the ZnS bandgap [16]. As a result, its photo reaction feedback rises. Among various transition metals, Co shifts the bandgap of ZnS in the visible region very effectively and how much Co can have done, it is our main investigation of this study.

Various techniques have been applied to fabricate semiconducting nanomaterials in the form of powder. Out of these synthetic methods, chemical precipitation process will be recognized to be the most useful due to its ease and simplicity. The chemical method usually required simple lab types of equipment, ambient environmental conditions, and the experiment complete within hours, whereas other methods often required sophisticated equipment, extreme environmental conditions (temperature, pressure, etc.) and large time intervals. The particle sizes and stability are controlled either by restricting the reaction space within matrices or by using stabilizers and capping agents.

In this study, we have reported structural and optical properties of chemically synthesized cobalt doped ZnS nanoparticles. To control the size of the nanoparticles we have used EDTA ($C_{10}H_{16}N_2O_8$) as a capping agent.

2. Experimental Setup

The Co-doped and undoped ZnS nanocrystals were prepared by chemical precipitation reaction due to its ease and simplicity. Zinc acetate [$Zn(CH_3COO)_2 \cdot 2H_2O$], sodium sulfide ($Na_2S$), cobalt chloride ($CoCl_2$), and EDTA were used as source materials. EDTA acted as the capping agent and deionized water was used as a solvent. All chemicals were of analytical grade.

Appropriate amount (calculated from stoichiometric ratio) of zinc acetate, sodium sulfide and cobalt chloride were dissolved in 100 mL deionized water by continuously stirring for 60 minutes to get 1 M solution separately at room temperature (30 °C). These three solutions with EDTA were mixed to get six different compositions (0.0, 0.1, 0.3, 0.5, 0.7 and 1.0%) of ZnS.

In this synthesis process, all the doped solutions have been centrifuged for 25 min in maximum speed 3,000 rpm. The obtained solution was centrifuged to separate ZnS powder. These nanocrystals of ZnS were repeatedly washed with ethanol and filtrate. The obtained ZnS was subsequently dried in an oven at 50 °C for 12 hours. To get fine grain powders to maximize surface area, to reduce particle size and to get a homogeneous mixture, powder was milled.

3. Experimental Results

3.1 Structural Analysis

Structural characterization and phase identification of nanocrystalline powder were carried out using GBC EMMA X-ray diffractometer with monochromatic Cu-Kα radiation ($\lambda = 1.5406$ Å) in a 2θ range.

X-ray diffraction pattern gives the information about crystalline structure and grain size of the nanoparticles. Fig. 1a shows the XRD patterns of the doped and undoped ZnS nanoparticles. There were three major diffraction peaks at 2θ values 28.60°, 47.60° and 56.50°. The peaks are appearing due to reflection from the (111), (220) and (311) planes of the cubic
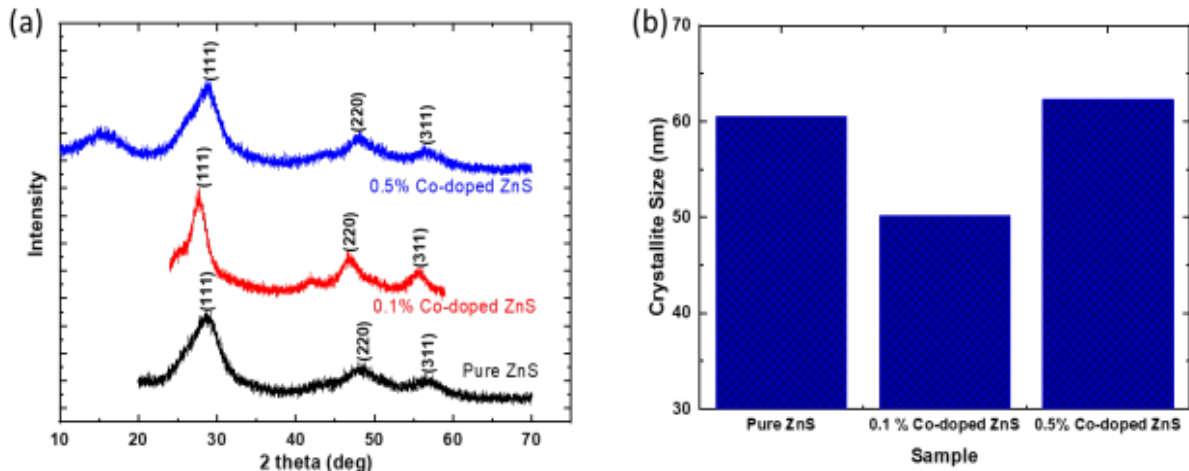
Fig. 1 (a) X-ray diffraction patterns of Co-doped ZnS nanoparticles, and (b) variation of crystallite size with cobalt content.

phase of the ZnS. The XRD pattern of the prepared samples is well matched with the standard cubic ZnS.

The diffraction peaks are significantly broadened due to the very small size of the nanocrystals [17]. No diffraction peaks corresponding to cobalt precipitates or cobalt-related impurity phase were detected, which further confirmed the formation of ZnS:Co solid solution instead of Co^{2+} precipitation or second phase.

In addition, diffraction peaks of the doped ZnS nanocrystals shift a little toward high angle compared with those of undoped ZnS nanocrystals. This suggests that the cobalt ions substitute the zinc ions, resulting in reduced lattice constants. The lattice constant was estimated using the following formula.

$$a = \frac{\lambda}{2 \sin \theta} \sqrt{h^2 + k^2 + l^2}$$

where λ is the X-ray wavelength, θ is the Bragg angle, and the Miller index of the crystal plane is h, k, l. For $x = 0$, a was found to be 5.4024 Å, which is close to the reported value of cubic blende ZnS. Similarly, the lattice constant a for $x = 0.1$, 0.5 and 1% of Co was found to be 5.2942, 5.2445 and 5.1908 Å respectively. It is clear that the lattice constant of the Co-doped ZnS nanoparticles decreases with the increase of the Co^{2+} content. This can be explained by the fact that Co^{2+} (0.072 nm) has a smaller radius than Zn^{2+} (0.074 nm). Moreover, this also suggests that some Zn^{2+} sites were substituted by Co^{2+}. The average particle sizes of the

samples were estimated from the broadening of the diffraction peaks using the Debye-Scherrer equation [19]:

$$D = \frac{K\lambda}{\beta \cos \theta}$$

where D is the particle size, k a fixed number of 0.9, λ the X-ray wavelength, θ the Bragg's angle in radians, and B the full width at half maximum of the peak in radians.

From Fig. 1b, the average particle size of pure, 0.1% and 0.5% of Co concentration were found to be 60.51 nm, 50.17 nm and 62.31 nm respectively. It is clearly observed that, the average particle size of Co-doped ZnS decreases with the increasing of the cobalt concentration.

3.2 Optical Properties Study

The optical properties of the synthesized ZnS nanoparticles have been studied by the UV-visible spectroscopy. The absorption and transmittance are recorded with the variation of incident photon wavelength in the range from 190 nm to 1,100 nm with 1 nm wavelength step using UV-2800 spectrometer.

3.2.1 Absorption, Transmission and Reflectance Spectra

UV-Vis spectra for all the samples were taken in the absorption and transmission mode at room temperature. Figs. 2a-2c show UV-visible absorption,

transmission and reflectance spectra of the samples obtained under optimum condition while dispersed in methanol.

It was observed that absorption and transmission spectra illustrated a standard transmission with respect to the doping of Co concentration of above 80%. This sharp rise in transmission and fall in absorption close to the bottom line of absorption edge are the recognition of the better crystallinity [20]. The percentage of transmittance changed with the increase of doping concentration. It may be the discharged photon of absorption spectra that caused this type of fluctuation in the optical transmission of doped ZnS. The sharp drop in absorption at relatively short wavelengths compared to the bulk material is indicative of the formation of ZnS nanoparticles.

Reflectance of the surface of a substance is its effectiveness in reflecting radiant energy. It is the fraction of incident electromagnetic power that is reflected at an interface. The reflectance R of a material with transmittance (T) and absorbance (A) is given by the following relation [5],

$$R = 1 - (Te^A)^2$$

From Fig. 2c, it has shown that, the samples of different concentration represented some reflection peaks at 200-800 nm range, which are in order of band-to-band transition [21]. Two major peaks at around 536 nm and 840 nm were found for cobalt doped ZnS NPs. The appearance of some impurities like Co^{2+} can not be opposed in the beginning. Also few absorption peaks are shown in longer wavelength for the different concentration of samples. Probably
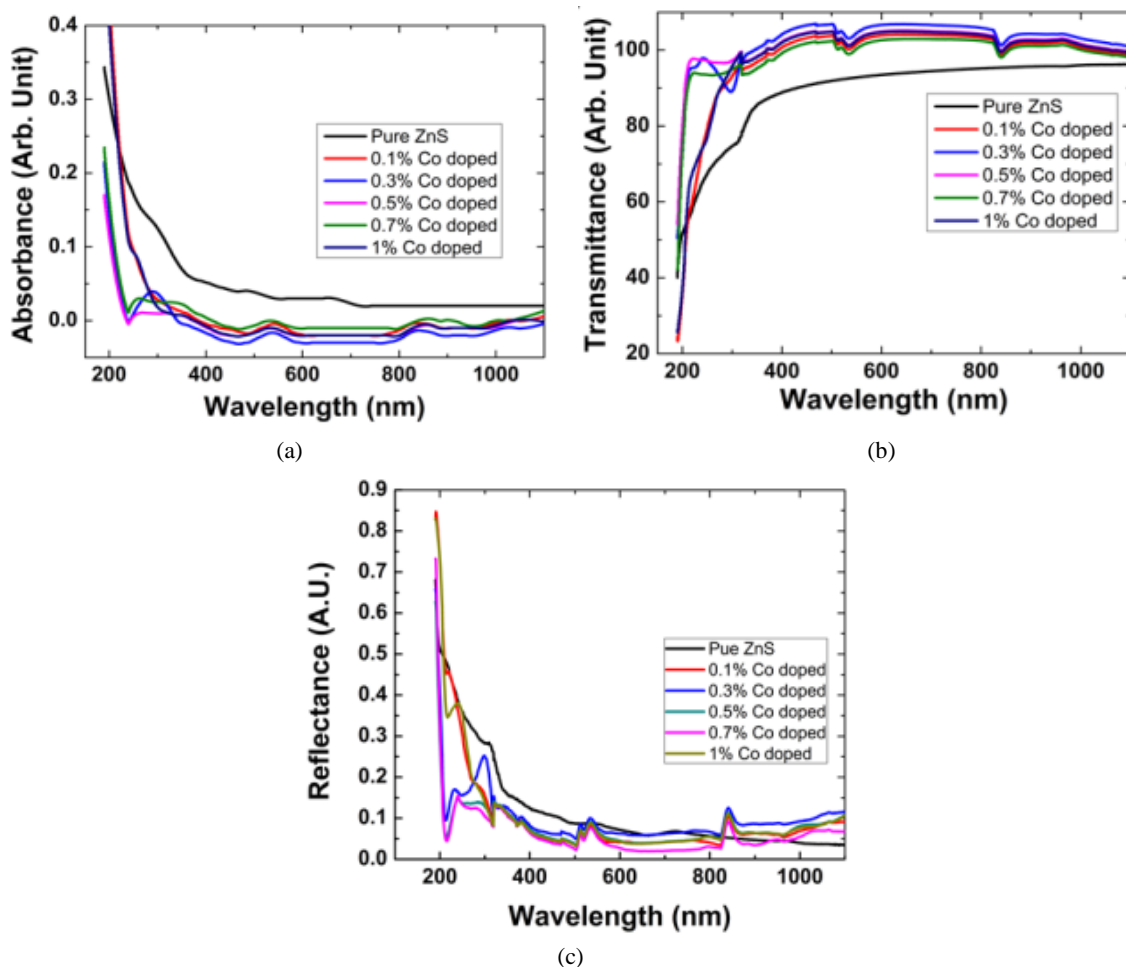

(a)

(b)

(c)

Fig. 2   UV-Vis (a) absorption, (b) transmission and (c) reflectance spectra of cobalt-doped ZnS nanoparticles at room temperature.

(a)   (b)
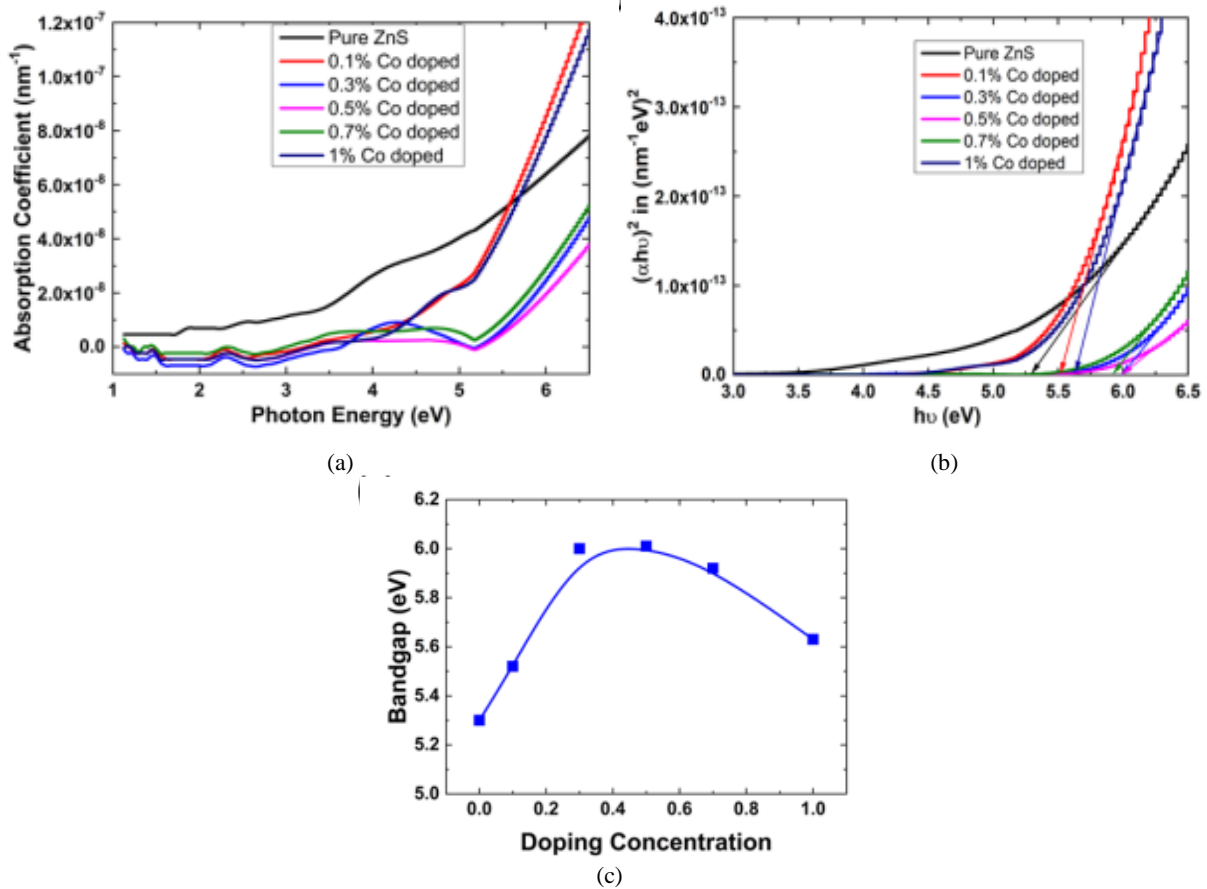

(c)

Fig. 3   (a) Absorption coefficient increases with photon energy; (b) bandgap determination from Tauc plots; (c) variation of bandgap with doping concentration.

these happened in order of sulfur contamination [22, 23].

3.2.2 Absorption Coefficient and Bandgap

The absorption coefficient of the samples was determined from the transmittance data using the following equation [24]:

$$\alpha = \frac{2.303\,A}{t}$$

where, T is the transmittance and t is the thickness of the sample holder.

Absorption coefficient (α) has been plotted against incident photon energy ($h\upsilon$) as shown in Fig. 3a. It was seen that the fall of absorption coefficient with decreasing photon energy at the band edge is slightly different from the sample which is synthesized at room temperature.

The bandgap of pure ZnS and Co-doped ZnS at different concentrations is obtained from this formula

[25]:

$$(\alpha h\upsilon)^2 = A\,(h\upsilon - E_g)$$

From Fig. 3b of $(\alpha h\upsilon)^2$ vs. energy (eV), it can be observed that, bandgap increases with respect to the doping concentration of Co content in the range of 5.30 eV-6.01 eV as tabulated in Table 1 and after a certain concentration it decreases (Fig. 3c). That is, bandgap saturated at a maximum value of 6.01 eV for 0.5% cobalt doped ZnS NPs. However, bandgap energy is affected by some factors such as—grain size, concentration of materials, stoichiometry fluctuations, appearance of impurities, temperature, etc. [26]. The illustration of higher bandgap energy at lower concentration of Co doping probably is the result of the smaller grain size of the nanoparticles.

Moreover, those observed higher bandgaps have controlled relation with the concentration of cobalt in ZnS NPs.

Table 1 Some determined optical parameters for cobalt doped ZnS NPs. Refractive indices and dielectric constants are measured for 590 nm incident photon wavelength.

ZnS sample	Optical bandgap (eV)	Refractive index (n)	Dielectric constant (ε_r)
Pure ZnS	5.30	1.75216	3.07007
0.1% Co-doped	5.52	1.51993	2.31018
0.3% Co-doped	6.00	1.67489	2.80526
0.5% Co-doped	6.01	1.55704	2.42437
0.7% Co-doped	5.92	1.42152	2.02073
1% Co-doped	5.63	1.53817	2.36596

3.2.3 Extinction Coefficient and Refractive Index

Extinction coefficient refers to several different measures of the absorption of light in a medium. The extinction coefficient of the nanoparticles was calculated using the relation [27]:

$$k = \frac{\alpha\lambda}{4\pi}$$

where α is the absorption coefficient and λ is the wavelength of the incident photon.

The variation of extinction coefficient against photon energy with different synthesized at room temperature is shown in Fig. 4a. It is observed that the plots of extinction coefficient indicate a decrease in the extinction coefficient with photon energy for samples. It also showed random dispersion pattern due to an excitation band [28]. Moreover, the noticeable variation of extinction coefficient of pure ZnS observed respect to the other samples may be in order of the crystallographic fluctuations like grain boundaries of the nanoparticles.

The refractive index of a material is a dimension less number that describes how light propagates through that medium. The refractive index determines how much the path of light is bent. The refractive index (η) of the nanoparticles was calculated from the following equation [20].

$$n = \frac{(1+R)}{(1-R)} + \left(\frac{4R}{(1-R)^2} - k^2\right)^{1/2}$$

where R is the reflectance and k is the extinction coefficient. It can be observed from Fig. 4b that, n_{max} value of pure ZnS is varied greatly from the other doped samples in the range of 200-300 nm wavelengths. Undoped ZnS NPs exhibited the highest refractive index at 590 nm and minimum for 0.7% cobalt containing ZnS.
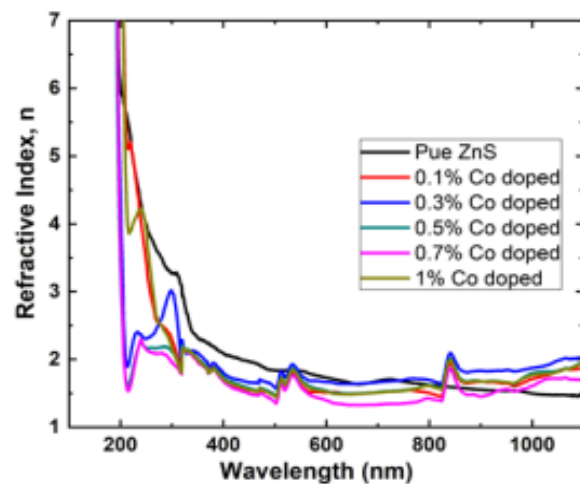
3.2.4 Dielectric Constants

The dielectric constant of the material is a quantity related to the refractive index. It is a measure of insulation. The dielectric constant of ZnS nanoparticles can be expressed by the relation [29]:

$$\varepsilon = \varepsilon_r + i\varepsilon_i$$

where ε_r and ε_i are the real and imaginary parts of the dielectric constant respectively. The real and imaginary parts of the dielectric constants can be calculated with the equations below:
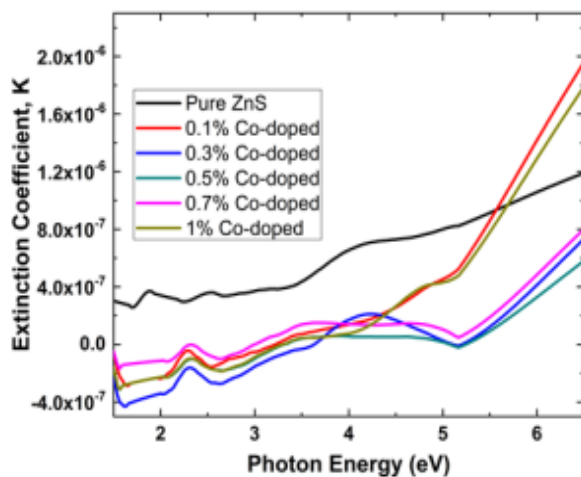
(a)   (b)

Fig. 4 (a) Variation of extinction coefficient with incident photon energy; (b) refractive index variation of Co-doped ZnS nanoparticles with pure ZnS nanoparticles.

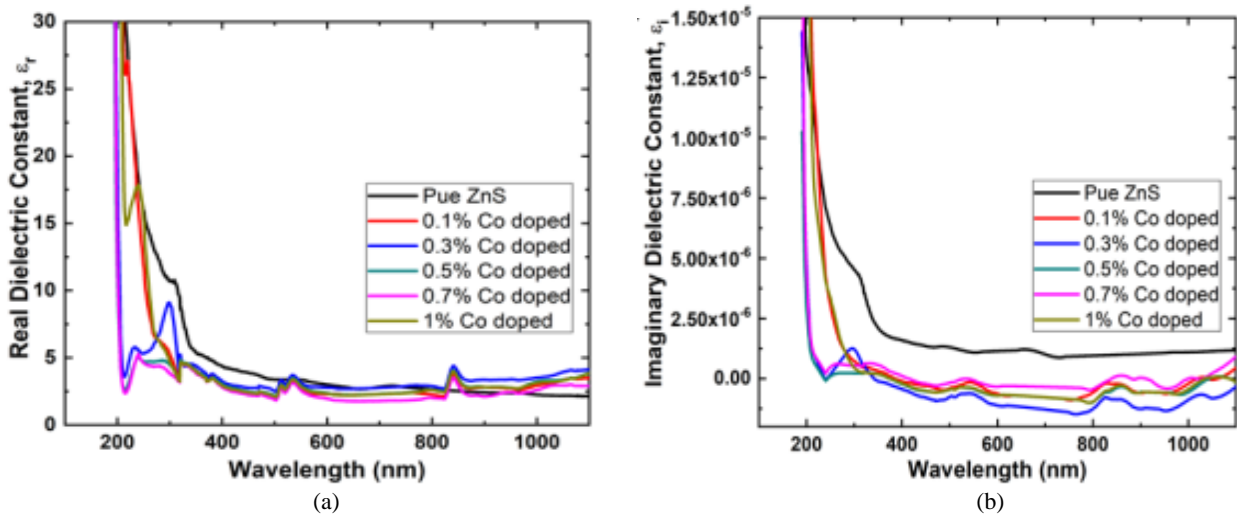(a)   (b)

Fig. 5 (a) Real dielectric constant, and (b) imaginary dielectric constant of Co-doped ZnS nanoparticles as a function of incident photon wavelength at room temperature.

$$\varepsilon_r = n^2 - k^2$$
$$\varepsilon_i = 2nk$$

From Figs. 5a and 5b it is observed that, real and imaginary dielectric constants were varied at a limited range. Moreover, dielectric constant changes with temperature [30] for the construction of their grain boundaries, but in this report we keep the temperature constant. So little variation happened probably. Undoped ZnS has the maximum dielectric constant.

4. Conclusions

ZnS nanoparticles doped with transition metal (Co) were successively synthesized by a simple chemical precipitation method. These nanoparticles were characterized structurally by XRD and found to have a cubic crystal structure with the diffraction peaks as (111), (220), and (311). The crystallite sizes of the undoped and doped ZnS nanoparticles have been calculated using Debye Scherrer's formula, which shows that crystallite size decreases as the molar concentration of dopant increases. The optical band gap values for undoped and doped ZnS nanoparticles have been calculated from the Tauc plot and it was found to be saturated at 6.01 eV for 0.5% cobalt containing ZnS NPs. It shows that the band gap of ZnS increases as the concentration of dopant increases. The results reveal that the synthesized ZnS

nanoparticles have the promising applications in optoelectronics.

References

[1] Cheng, Z. H., et al. 1998. "Structure, Exchange Interactions, and Magnetic Phase Transition of Intermetallic Compounds." *Phys. Rev. B-Condens. Matter Mater. Phys.* 57 (22): 14299-309.

[2] Mahdi, H. S., Parveen, A., and Azam, A. 2018. "Structural and Photoluminescence Properties of Ni Doped CdS Nanoparticles Synthesis by Sol Gel Method." *AIP Conf. Proc.* 1953.

[3] Bi, C., et al. 2010. "Facile Fabrication of Wurtzite ZnS Hollow Nanospheres Using Polystyrene Spheres as Templates." *Mater. Lett.* 64 (15): 1681-3.

[4] Poornaprakash, B., Amaranatha Reddy, D., Murali, G., Madhusudhana Rao, N., Vijayalakshmi, R. P., and Reddy, B. K. 2013. "Composition Dependent Room Temperature Ferromagnetism and PL Intensity of Cobalt Doped ZnS Nanoparticles." *J. Alloys Compd.* 577: 79-85.

[5] Harish, G. S., and Sreedhara Reddy, P. 2015. "Synthesis and Characterization of Ce, Cu Co-Doped ZnS Nanoparticles." *Phys. B Condens. Matter* 473: 48-53.

[6] Bhargavaa, R. N., Gallaghera, D., and Welkerb, T. 1994. "Doped Nanocrystals of Semiconductors—A New Class of Luminescent Materials." *Journal of Luminescence* 61: 275-80.

[7] Wang, Y., and Herron, N. 1991. "Nanometer-Sized Semiconductor Clusters: Materials Synthesis, Quantum Size Effects, and Photophysical Properties." *J. Phys. Chem.* 95 (2): 525-32.

[8] Godlewski, M., Surma, M., Ivanov, V. Y., and Surkova, T. P. 2004. "Mechanisms of Radiative and Nonradiative

Recombination in ZnSe:Cr and ZnSe:Fe." *Low Temp. Phys.* 30 (11): 891-6.

[9] Li, J., et al. 2006. "Enhanced Ultraviolet Emission from ZnS-Coated ZnO Nanowires Fabricated by Self-Assembling Method." *J. Phys. Chem. B* 110 (30): 14685-7.

[10] Boyn, R. 1988. "4f-4f Luminescence of Rare-Earth Centers in II-VI Compounds." *Phys. Status Solidi* 148 (1): 11-47.

[11] Peka, P., and Schulz, H. J. 1994. "Empirical One-Electron Model of Optical Transitions in Cu-Doped ZnS and CdS." *Phys. B Phys. Condens. Matter* 193 (1): 57-65.

[12] Ayim-Otu, B., Kuncan, M., Şahin, Ö., and Horoz, S. 2020. "Synthesis and Photovoltaic Application of ZnS:Cu (3%) Nanoparticles." *J. Aust. Ceram. Soc.* 56 (2): 639-43.

[13] Liu, S. M., Guo, H. Q., Zhang, Z. H., Liu, F. Q., and Wang, Z. G. 2000. "Photoluminescence of Eu^{2+} Doped ZnS Nanocrystals." *Chinese Physics Letters* 17 (8): 609-11.

[14] Sarkar, R., Tiwary, C. S., Kumbhakar, P., Basu, S., and Mitra, A. K. 2008. "Yellow-Orange Light Emission from Mn^{2+}-Doped ZnS Nanoparticles." *Phys. E Low-Dimensional Syst. Nanostructures* 40 (10): 3115-20.

[15] Kamal, C. S., Mishra, R. K., Patel, D. K., Rao, K. R., Sudarsan, V., and Vatsa, R. K. 2016. "Effect of Structure, Size and Copper Doping on the Luminescence Properties of ZnS." *Mater. Res. Bull.* 81: 127-33.

[16] Jiang, P., Xiang, W., Kuang, J., Liu, W., and Cao, W. 2015. "Effect of Cobalt Doping on the Electronic, Optical and Photocatalytic Properties of TiO_2." *Solid State Sci.* 46: 27-32.

[17] Sharma, R. K., Kumar, A., Gautam, S., and Goyal, N. 2016. "Synthesis and Characterization of Cobalt Doped ZnS Nanoparticles." *Integrated Research Advances* 3 (1): 26-9.

[18] Cullity, B. D. 1978. *Elements of X-ray Diffraction,* 2nd Ed. Manila, Philippines: Addison-Wesley, 324-39.

[19] Alexander, L., and Klug, H. P. 1950. "Determination of Crystallite Size with the X-ray Spectrometer." *J. Appl. Phys.* 21 (2): 137-42.

[20] Jothibas, M., Johnson Jeyakumar, S., Manoharan, C., Kartharinal Punithavathy, I., Praveen, P., and Prince Richard, J. 2017. "Structural and Optical Properties of Zinc Sulphide Nanoparticles Synthesized via Solid State Reaction Method." *J. Mater. Sci. Mater. Electron.* 28 (2): 1889-94.

[21] Borah, J. P., and Sarma, K. C. 2008. "Optical and Optoelectronic Properties of ZnS Nanostructured Thin Film." *Acta Phys. Pol. A* 114 (4): 713-9.

[22] Clauser, C., and Huenges, E. 2013. "Rock Physics & Phase Relations: A Handbook of Physical Constants." In *Thermal Conductivity of Rocks and Minerals*, pp. 105-26.

[23] Annapurna, K., Kumar, A., Dwivedi, R. N., Hussain, N. S., and Buddhudu, S. 2000. "Fluorescence Spectra of Cu^+: ZnO-B_2O_3-SiO_2 Glass." *Mater. Lett.* 45 (1): 23-6.

[24] Dehghani, Z., Nazerdeylami, S., Saievar-Iranizad, E., and Majles Ara, M. H. 2011. "Synthesis and Investigation of Nonlinear Optical Properties of Semiconductor ZnS Nanoparticles." *J. Phys. Chem. Solids* 72 (9): 1008-10.

[25] Sarkar, R., Tiwary, C. S., Kumbhakar, P., and Mitra, A. K. 2009. "Enhanced Visible Light Emission from Co^{2+} Doped ZnS Nanoparticles." *Phys. B Condens. Matter* 404 (21): 3855-8.

[26] Pattabi, M., and Uchil, J. 2000. "Synthesis of Cadmium Sulphide Nanoparticles." *Sol. Energy Mater. Sol. Cells* 63 (4): 309-14.

[27] Sridhar, R., Manoharan, C., Ramalingam, S., Dhanapandian, S., and Bououdina, M. 2014. "Spectroscopic Study and Optical and Electrical Properties of Ti-Doped ZnO Thin Films by Spray Pyrolysis." *Spectrochim. Acta-Part A Mol. Biomol. Spectrosc.* 120: 297-303.

[28] Coogan, C. K. 1957. "The Measurement of the Optical Properties of Zinc Sulphide." *Proc. Phys. Soc. Sect. B* 70 (9): 845-61.

[29] Suresh, S. 2013. "Synthesis, Structural and Dielectric Properties of Zinc Sulfide Nanoparticles." *Int. J. Phys. Sci.* 8 (21): 1121-7.

[30] Mukherjee, S., Chen, C. H., Chou, C. C., and Yang, H. D. 2010. "Anomalous Dielectric Behavior in Nanoparticle Eu_2O_3:SiO_2 Glass Composite System." *Europhys. Lett.* 92 (5).